

Syntheses and Performance of layered $\text{LiNi}_x\text{Co}_{1-2x}\text{Mn}_x\text{O}_2$ as Cathode Materials for Lithium-Ion Batteries

Zhao Jin, Xinyu Jiang, Xiangzhe Liu, Xin Wang, Jinhua Luo, and Jijun Feng*

Key Laboratory of Chemical Sensing & Analysis in Universities of Shandong, School of Chemistry and Chemical Engineering, University of Jinan, Jinan 250022, China

*lab_feng@163.com

Keywords: Lithium-ion batteries, Cathode material, $\text{LiCo}_{1-2x}\text{Ni}_x\text{Mn}_x\text{O}_2$, Metal acetate decomposition

Abstract. The layered cathode materials $\text{LiNi}_x\text{Co}_{1-2x}\text{Mn}_x\text{O}_2$ ($x=1/11, 2/11, 3/11, 4/11, 5/11$) powders for lithium-ion batteries were synthesized by metal acetate decomposition technique. The evolution of the structural properties and electrochemical performances of $\text{LiNi}_x\text{Co}_{1-2x}\text{Mn}_x\text{O}_2$ with Co content decreased were investigated by X-ray diffraction (XRD) and rietveld refinement, scanning electronic microscopy (SEM) and galvanostatic charge and discharge cycle. The results showed that the appropriate substitution of Co by Ni, Mn could greatly improve the performances of the as-prepared materials in capacity, initial columbic efficiency, rate ability and cycle capability. Among the series of materials, the optimal performance belonged to $\text{LiNi}_{3/11}\text{Co}_{5/11}\text{Mn}_{3/11}\text{O}_2$, which delivered an initial discharge capacity of $157.6 \text{ mAh}\cdot\text{g}^{-1}$ and preserved $150.4 \text{ mAh}\cdot\text{g}^{-1}$ after 30 cycles in the voltage range of $2.5 \sim 4.3 \text{ V}$ at 0.2 C . Comparative cycle data at 0.5 C and 1.0 C were presented implying that the $\text{LiNi}_{3/11}\text{Co}_{5/11}\text{Mn}_{3/11}\text{O}_2$ also had a significantly improvement in rate capability.

Introduction

Lithium-ion batteries (LIB) have been widely used in portable appliances, consumer electronics and hybrid electric vehicles^[1] because of their excellent performances, especially the high specific energy. However, several disadvantageous features or dissatisfying properties have restricted the fields of applications, such as cathode materials.^[2] Different kinds of cathode materials such as LiCoO_2 , LiNiO_2 , LiMnO_2 , LiMn_2O_4 , LiFePO_4 ,^[3] vanadium oxide^[4] and their derivatives have been studied^[5,6]. Recently, layered $\text{LiNi}_x\text{Co}_{1-2x}\text{Mn}_x\text{O}_2$ transition metal mixed oxides, which can undergo oxidation to higher valences when lithium ion is removed^[5,6] become the research focus due to their higher capacity, better safety and “greener”^[7-9] compared with commercial LiCoO_2 . The mixed oxides retain the virtue of mono metal oxide such as good cycling performance of LiCoO_2 ^[10], high capacity delivery of LiNiO_2 ^[11], and super safety of LiMn_2O_4 ^[12]. At the same time, the mixed oxides conquer their shortcomings, including the cost and environmental pollution problems of LiCoO_2 , bad stability and order of LiNiO_2 , slow fading capacity of LiMn_2O_4 , relatively low voltages (typically 3 V or less) of vanadium oxide.

Recently, intensive effort has been directed to improve the electrochemical performance of the $\text{LiNi}_x\text{Co}_{1-2x}\text{Mn}_x\text{O}_2$, especially the cycle performance and thermal stability. New outstanding preparation methods have been extensively investigated, such as sol-gel method, co-precipitation method^[13], hydrothermal method^[14] and chemical vapor deposition method^[15]. Commercially, material powders are usually prepared via high-temperature solid-state reaction of mechanically mixed lithium compounds and transition metals oxides, but they are energy intensive and can't readily produce potentially metastable structures that might result in high lithium ion diffusivity. Method of metal acetate decomposition has been reported to compose the oxides of transition metals in a few literatures.^[16] Compared to sol-gel method, co-precipitation method and so on, this method is simpler and “greener”, because the entire reaction does not require water or other solvent and generates no wastewater and sludge.

The aim of this work was to synthesize a series of layered multi-components materials $\text{LiNi}_x\text{Co}_{1-2x}\text{Mn}_x\text{O}_2$ ($x=1/11, 2/11, 3/11, 4/11, 5/11$) via the metal acetate decomposition method. Based on the powder X-ray Diffraction, we could refine the typical crystal structure of samples and the

morphology was characterized using scanning electron microscopy. Meanwhile, their electrochemical properties were systematically investigated and compared by means of the charge and discharge experiments.

Experimental

The raw materials of the aimed samples were analytically pure $\text{LiOH}\cdot\text{H}_2\text{O}$, $\text{C}_2\text{H}_2\text{O}_4\cdot 2\text{H}_2\text{O}$, $\text{Co}(\text{CH}_3\text{COO})_2\cdot 4\text{H}_2\text{O}$, $\text{Ni}(\text{CH}_3\text{COO})_2\cdot 4\text{H}_2\text{O}$ and $\text{Mn}(\text{CH}_3\text{COO})_2\cdot 4\text{H}_2\text{O}$. Stoichiometrically weighted $\text{LiOH}\cdot\text{H}_2\text{O}$ and $\text{C}_2\text{H}_2\text{O}_4\cdot 2\text{H}_2\text{O}$ were mixed and skived in a agate mortar followed by stoichiometrically weighted $\text{Co}(\text{CH}_3\text{COO})_2\cdot 4\text{H}_2\text{O}$, $\text{Ni}(\text{CH}_3\text{COO})_2\cdot 4\text{H}_2\text{O}$ and $\text{Mn}(\text{CH}_3\text{COO})_2\cdot 4\text{H}_2\text{O}$ to get the pink mixture. The obtained mixture was then dried in a vacuum dryer at $150\text{ }^\circ\text{C}$ for 12 h to gain the precursor. The precursor was then preburned at $350\text{ }^\circ\text{C}$ for 4 h. After natural cooling, the precursor were skived in agate mortar and then pressed at 10 Mpa. The gained wafers were heat-treated at $800\text{ }^\circ\text{C}$ for 15 h and temper-treated at $600\text{ }^\circ\text{C}$ for 2 h. The black samples were finally prepared after natural cooling in the furnace and skived in agate mortar.

X-ray diffraction patterns of the $\text{LiNi}_x\text{Co}_{1-2x}\text{Mn}_x\text{O}_2$ ($x=1/11, 2/11, 3/11, 4/11, 5/11$) powder samples were recorded using a Bruker AXS D8 Advance X-ray Diffractometer with $\text{Cu K}\alpha$ radiation in the 2θ range of $10\text{--}80^\circ$. Morphology of the samples was observed on the Hitachi S-2500 Scanning Electron Microscope. The charge and discharge behaviors were examined using CR2032 coin-type cells on PCBT-138-32D battery program-control test system. The cathode consisted of the synthesized cathode material (80 wt. %), acetylene black (12 wt. %) and polytetrafluoroethylene (PTFE) (8 wt. %). The prepared slurry was coated onto an aluminum foil, pressed at 10 MPa, and then vacuum dried at $120\text{ }^\circ\text{C}$ for 12 h. Besides the fabricated cathodes, the cells were made up of lithium metal pellets as anode, $1\text{ mol}\cdot\text{L}^{-1}\text{ LiPF}_6$ in EC+DMC (1: 1 volume ratio) as electrolytes and celgard 2300 membrane as separators. All cells were assembled in an argon-filled glove box (Mikrouna Super 1220/750/900). The galvanostatical charge-discharge tests were performed between 2.5 and 4.3 V (vs. Li/Li^+) with the current density of 0.2 C in the first 30 cycles, and then 10 cycles at 0.5 C, followed by 3 cycles at 0.2 C, then 10 cycles at 1.0 C followed by 3 cycles at 0.2 C.

Results and discussion

Crystal structure

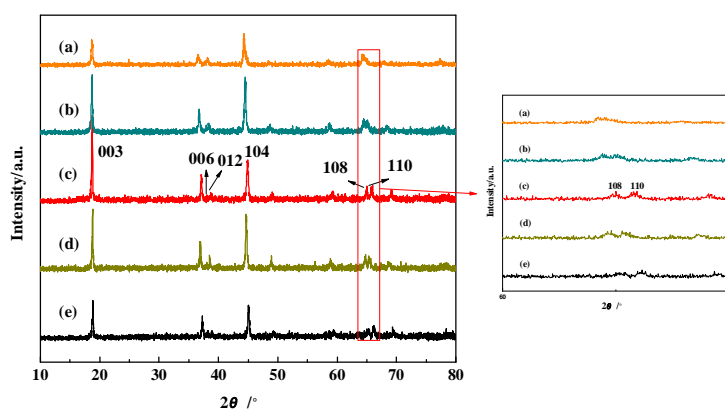


Fig. 1 XRD patterns of $\text{LiNi}_x\text{Co}_{1-2x}\text{Mn}_x\text{O}_2$ ($x=1/11, 2/11, 3/11, 4/11, 5/11$) samples (a) $\text{LiNi}_{5/11}\text{Co}_{1/11}\text{Mn}_{5/11}\text{O}_2$; (b) $\text{LiNi}_{4/11}\text{Co}_{3/11}\text{Mn}_{4/11}\text{O}_2$; (c) $\text{LiNi}_{3/11}\text{Co}_{5/11}\text{Mn}_{3/11}\text{O}_2$; (d) $\text{LiNi}_{2/11}\text{Co}_{7/10}\text{Mn}_{2/11}\text{O}_2$; (e) $\text{LiNi}_{1/11}\text{Co}_{9/11}\text{Mn}_{1/11}\text{O}_2$

As shown in Fig. 1, the XRD patterns of the prepared powders reveal that all diffraction peaks are indexed based on the $\alpha\text{-NaFeO}_2$ structure with R-3m space group, with no impurity phase detected,

suggesting that these materials prepared under our condition are well-crystallized. Especially, the peaks of $\text{Li Ni}_{3/11}\text{Co}_{5/11}\text{Mn}_{3/11}\text{O}_2$ are sharper and narrower. Besides, its clearly splitting of (006)/(012) and (108)/(110) doublet, just as right of Fig. 1, indicates that substitution of Ni, Mn for some amount of Co can lead to ideal layered structure. The refined structural parameters showed that all the samples have the shifts of 2θ to smaller values and the width peaks with larger values of full width at half peak (FWHP) have risen with the increasing Ni, Mn content. The intensity ratio of (003)/(104) peaks can be used to determine the cation distribution in the lattice. The higher this ratio is, the lower degree of the cation mixing shall be. The higher value of 1.5083 for $\text{Li Ni}_{3/11}\text{Co}_{5/11}\text{Mn}_{3/11}\text{O}_2$ explains a lower cation mixing. Furthermore, with the increasing Ni, Mn substitution, the lattice parameters become larger both in the a- and c-directions, bringing lattice volume expansion. This is propitious to keep the structure of the compounds more stable when Li^+ inserts or extracts. Stable structure will result in perfect electrochemical performance.

Morphology

SEM micrographs of $\text{Li Ni}_{3/11}\text{Co}_{5/11}\text{Mn}_{3/11}\text{O}_2$ sample at different magnifications were shown in Fig. 2. It can be seen from the figures that the product consists of particles whose size is about $1\ \mu\text{m}$ and some larger aggregations. Both particles and aggregations show clear surface and slick edge. At the same time, the particle distribution is well-proportioned. High specific capacity and good cycling ability may root in the excellent surface and particle size character of the material because of their effect on the intercalation process of Li^+ ion.

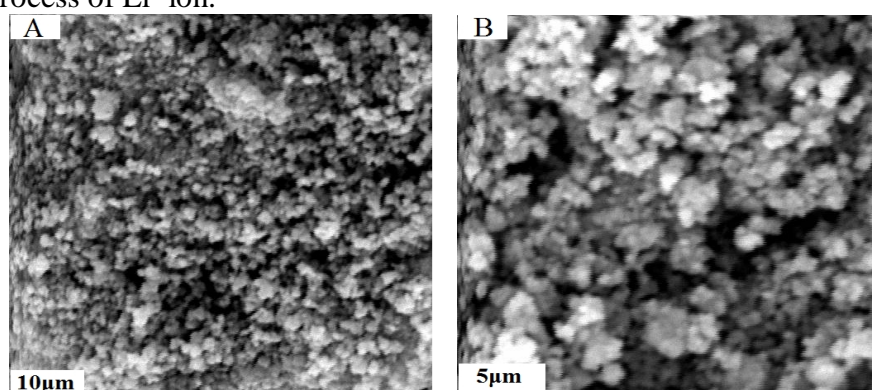


Fig. 2 SEM images of synthesized $\text{Li Ni}_{3/11}\text{Co}_{5/11}\text{Mn}_{3/11}\text{O}_2$ at different magnifications

Electrochemical evaluation

Fig. 3(a) compared the initial charge-discharge curves of the $\text{LiNi}_x\text{Co}_{1-2x}\text{Mn}_x\text{O}_2$ ($x=1/11, 2/11, 3/11, 4/11, 5/11$) with current rate of 0.2 C between 2.5 and 4.3 V at room temperature. It can be seen in Fig. 3 that all the curves are quite smooth without any plateau, which implies that no spinel-related phases are formed during charging and discharging. $\text{Li Ni}_{3/11}\text{Co}_{5/11}\text{Mn}_{3/11}\text{O}_2$ has a higher charge capacity of $172.0\ \text{mAh}\cdot\text{g}^{-1}$ and delivers a larger initial discharge capacity of $157.6\ \text{mAh}\cdot\text{g}^{-1}$, whose irreversible capacity is $14.4\ \text{mAh}\cdot\text{g}^{-1}$. In addition, compared to others, $\text{Li Ni}_{3/11}\text{Co}_{5/11}\text{Mn}_{3/11}\text{O}_2$ exhibits a more outstanding charge/discharge efficiency of 91.63%. The larger discharge capacity may be explained by the electron exchange between transition metal ion and oxygen.³¹

The specific discharge capacities of $\text{LiNi}_x\text{Co}_{1-2x}\text{Mn}_x\text{O}_2$ ($x=1/11, 2/11, 3/11, 4/11, 5/11$) as functions of cycle numbers were exhibited in Fig. 3 (b). The cells were cycled between 2.5 and 4.3 V at various charge/discharge current densities of 0.2 C 30 cycles, 0.5 C 10 cycles, 0.2 C 3 cycles, 1.0 C 10 cycles and 0.2 C 3 cycles at room temperature. Remarkably different cycle performance among all the samples can be easily seen from Fig. 4. $\text{LiNi}_{3/11}\text{Co}_{5/11}\text{Mn}_{3/11}\text{O}_2$ shows a higher specific discharge capacity with better cycling stability compared to other samples. At 0.2 C rate, the initial specific discharge capacity is $157.6\ \text{mAh}\cdot\text{g}^{-1}$ for sample $\text{LiNi}_{3/11}\text{Co}_{5/11}\text{Mn}_{3/11}\text{O}_2$, and the reversible specific discharge capacities after 30 cycles is $150.4\ \text{mAh}\cdot\text{g}^{-1}$ (95.4% of the initial capacity). The discharge capacity decrease from 135.6 to $134.8\ \text{mAh}\cdot\text{g}^{-1}$ at 0.5 C rate, with only 0.08% capacity loss per cycle, while at 1.0 C rate 0.10% capacity fade per cycle. Furthermore, the $\text{LiNi}_{3/11}\text{Co}_{5/11}\text{Mn}_{3/11}\text{O}_2$ cathode keeps higher charge-discharge efficiencies of about 98% in the first 30 cycles and no less than 94% in the succedent

cycles, more excellent than others. Both the specific discharge capacities and efficiencies reveal the excellent capacity retention ability of sample $\text{LiCo}_{5/11}\text{Ni}_{3/11}\text{Mn}_{3/11}\text{O}_2$. This may be attributed to the fact that the appropriate Ni, Mn substitution can effectively restrain the nonstoichiometric products and bring on more ordered layered structure. The result is in agreement with the XRD analysis.

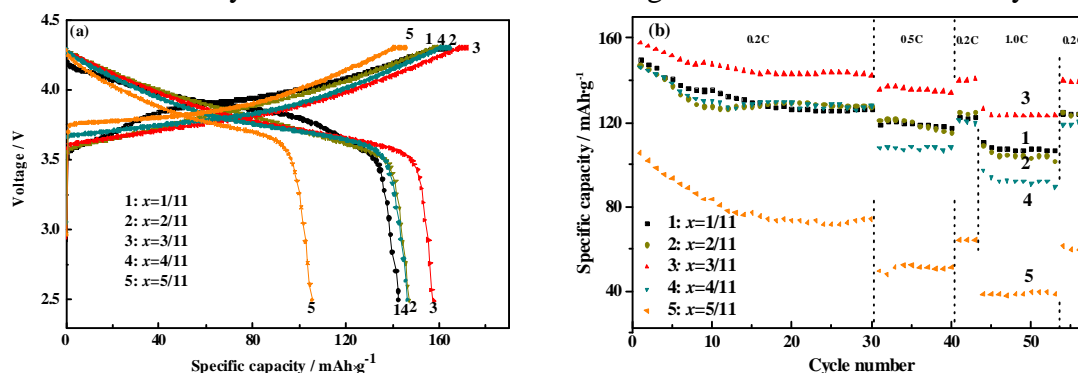


Fig. 3 (a) Initial charge-discharge curves and (b) cycle performance of $\text{LiNi}_x\text{Co}_{1-2x}\text{Mn}_x\text{O}_2$ at 0.2 C rate

Conclusions

The layered $\text{LiNi}_x\text{Co}_{1-2x}\text{Mn}_x\text{O}_2$ ($x=1/11, 2/11, 3/11, 4/11, 5/11$) cathode materials had been synthesized by the metal acetate decomposition method. All samples were proved as single-phase layered structure. Substitution of Co by Ni, Mn could effectively restrain the nonstoichiometric products and improve the electrochemical properties. Among the series of materials, $\text{LiNi}_{3/11}\text{Co}_{5/11}\text{Mn}_{3/11}\text{O}_2$ exhibited the most excellent electrochemical property. After 30 cycles at 0.2 C, its discharge capacity and capacity retention ratio were $150.4 \text{ mAh}\cdot\text{g}^{-1}$ and 96% apart, suggesting excellent cycling stability. The material $\text{LiNi}_{3/11}\text{Co}_{5/11}\text{Mn}_{3/11}\text{O}_2$ and other Ni-Co-Mn multiple materials are promising for application in lithium-ion batteries.

Acknowledgements

This work was financially supported by Natural Science Foundation of China (No. 51102114, 21201079) and Sci-Tech Development Project of Jinan (No. 201401234).

References

- [1] J. W. Fergus. J. Power Sources. Vol.195 (2010), p. 939
- [2] P. Y. Liao, J. G. Duh, S. R. Sheen. J. Power Sources. Vol.143 (2005), p. 212
- [3] A. Ritchie, W. Howard. J. Power Sources. Vol.162 (2006), p. 809
- [4] J. J. Feng, X. Z. Liu, X. Liu, et al. Chinese J. Inorg. Chem., Vol. 25 (2009), p. 001
- [5] Z. P. Huang, L. Y. Guo, C. Guo, et al. Acta Phys. Chim. Sin. Vol.31 (2015), p. 700
- [6] M. S. Whittingham. Chem. Rev. Vol.104 (2004), p. 4271
- [7] J. J. Feng, Z. P. Huang, C. Guo, et al. ACS Appl. Mater. Inter. Vol. 5 (2013), p. 10227
- [8] S. H. Park, C. S. Yoon, S. G. Kang, et al. Electrochim. Acta. Vol. 49 (2004), p. 557
- [9] T. H. Cho, Y. Shiosaki, H. J. Noguchi. Power Sources. Vol. 159 (2006), p. 1322
- [10] Z. Y. Tang, J. J. Feng. Acta Phys. Chim. Sin. Vol. 19 (2003), p. 1025
- [11] A. A. M. Prince, S. Mylswamy, C. Y. Wang, et al. Solid State Commun. Vol. 132 (2004), p. 273
- [12] B. L. He, W. J. Zhou, S. J. Bao, et al. Electrochim. Acta. Vol. 52 (2007), p. 3286
- [13] K. H. Dai, Y. T. Xie, Y. J. Wang, Z. S. Song. Electrochim. Acta. Vol. 53 (2008), p. 3257
- [14] J. J. Feng, X. Liu, X. Z. Liu, et al. Acta Phys. Chim. Sin. Vol. 25 (2009), p. 001
- [15] H. Jung, M. Park, S. H. Han, et al. Solid State Commun. Vol. 125 (2003), p. 387
- [16] X. Z. Liu, J. J. Feng, X. Liu. J. Univ. Jinan. [Sci.&Tech.]. Vol. 24 (2010), p. 364